



Evaluation of Anti-Inflammatory and Anticancer Activities of *Maerua angolensis* DC. Leaf Extract-Loaded Chitosan Nanoparticles

Cletus Anes Ukwubile^{✉,1,*}  Muhammad Zannah Lawan^{✉,2}  Troy Salvia Malgwi^{✉,1} 
Hassan Braimah Yesufu^{✉,3} 

¹ Department of Pharmacognosy, Faculty of Pharmacy, University of Maiduguri, Maiduguri P.M.B. 1069, Borno State, Nigeria

² Department of Chemical Engineering, Faculty of Engineering, University of Maiduguri, Maiduguri P.M.B. 1069, Borno State, Nigeria

³ Department of Pharmaceutical Chemistry, Faculty of Pharmacy, University of Maiduguri, Maiduguri P.M.B. 1069, Borno State, Nigeria

Article History

Submitted: February 07, 2025

Accepted: July 18, 2025

Published: August 15, 2025

Abstract

Background: Medicinal plants' bioactive compounds have emerged as promising alternatives, with *Maerua angolensis* gaining attention in Nigeria for its potential anti-cancer activity while being traditionally used for its anti-inflammatory properties. **Aim:** The study is designed to evaluate the anti-inflammatory and anti-cancer effects of the *M. angolensis* leaf extract incorporated into chitosan nanoparticles (MALC-NPs). **Methods:** During the study, chitosan nanoparticles were fabricated using the ionic gelation method, and later, the *M. angolensis* leaves were encapsulated in them. The dynamic light scattering (DLS), Fourier-transform infrared (FTIR) spectroscopy, and scanning electron microscopy (SEM) techniques were used to assess the physicochemical properties of MALC-NPs. The effectiveness of the anti-inflammatory activity was analyzed by measuring the amount of nitric oxide (NO) produced, and the activity of the cyclooxygenase-2 (COX-2) enzyme was measured. The MCF-7 (breast cancer) and A549 (lung cancer) cell lines were used to determine the cytotoxicity of MALC-NPs by MTT assay, while flow cytometry using Annexin V-FITC/PI staining reagents was performed to assess apoptosis induction. **Results:** MALC-NPs showed a particle size of 150 ± 5 nm, zeta potential of +32.6 mV, and an encapsulation efficiency of 86.4%, which indicates the stability of the nanoparticle and effective loading of the drug. In vitro assays showed greater anti-inflammatory activities, significant inhibition of NO production (IC_{50} : 21.5 μ g/mL) and COX-2 activity (IC_{50} : 18.7 μ g/mL) over time. The evaluation of cytotoxicity demonstrated the dose-dependent inhibition of MCF-7 (IC_{50} : 27.8 μ g/mL) and A549 (IC_{50} : 32.4 μ g/mL) carcinoma cells. Apoptosis induction was validated by flow cytometry. The early apoptosis values were 48.2% for MCF-7 and 41.7% for A549; late apoptosis values were 22.5% and 18.6%. **Conclusions:** These results demonstrate the possible anti-inflammatory and anticancer actions of *M. angolensis*-chitosan nanoparticles. Their ability to inhibit inflammatory mediators suggests their possible use as an alternative therapeutic agent for inflammation-malignancy associated cancers.

Keywords:

Maerua angolensis; chitosan nanoparticles; inflammation; apoptosis; breast cancer

1. Introduction

Chronic inflammation and cancer are among the most prevalent causes of death and disease in the modern world, impacting millions of patients each year. As stated by the World Health Organization, cancer is the second leading cause of death globally and continues to have rising inci-

dence rates due to alterations in lifestyles, environmental toxins, and heritable factors [1]. Chronic inflammatory diseases such as arthritis, Inflammatory Bowel Disease (IBD), and autoimmune disorders significantly deteriorate quality of life and contribute to increased healthcare costs. The increase in inflammatory markers within the body highlights the strong link between chronic inflamma-

* Corresponding Author:

Cletus Anes Ukwubile, Department of Pharmacognosy, Faculty of Pharmacy, University of Maiduguri, Maiduguri P.O. Box 1069, Borno State, Nigeria; caukwubile@unimaid.edu.ng



© 2025 Copyright by the Authors.

Licensed as an open access article using a [CC BY 4.0 license](https://creativecommons.org/licenses/by/4.0/).

tion and cancer development, as inflammation is the sole reason for starting, developing, and spreading tumors [2].

Inflammation represents a complex biological response to harmful stimuli, including infections, toxins, and tissue injury. Acute inflammation acts as a protective response that aids healing, yet chronic inflammation proves harmful because it generates oxidative stress and DNA damage while constantly activating inflammatory cytokines like tumor necrosis factor-alpha (TNF- α), interleukin-1 beta (IL-1 β), and cyclooxygenase-2 (COX-2) [3]. These pro-inflammatory mediators create a tumorigenic environment by fostering genetic mutations, uncontrolled cell proliferation, angiogenesis, and immune evasion [4]. This understanding has led researchers to explore therapeutic agents capable of simultaneously targeting both inflammatory pathways and cancer cells.

The treatment options currently used for cancer and inflammatory diseases include chemotherapy, radiotherapy, immunotherapy, and conventional NSAIDs. These treatments frequently face substantial limitations. Chemotherapy achieves positive results but produces intense side effects like myelosuppression, nephrotoxicity, and gastrointestinal toxicity, which restrict patient adherence to treatment protocols. NSAIDs, commonly used to treat inflammation, are linked to gastrointestinal ulcers, cardiovascular complications, and renal dysfunction when used over extended periods. Cancer therapy continues to confront the major obstacle of drug resistance, which drives the need for the development of more effective and safer treatment alternatives [5,6].

Maerua angolensis DC. (Capparaceae) is a medicinal plant widely used in African traditional medicine for treating pain, fever, wounds, and infections. The plant has been traditionally employed as an anti-inflammatory remedy, suggesting its potential use in managing chronic inflammatory disorders [7]. Several Phytochemical studies have identified a diverse range of bioactive compounds in *M. angolensis*, including flavonoids, alkaloids, terpenoids, and saponins, which exhibit potent anti-inflammatory and cytotoxic properties [7]. Flavonoids and alkaloids have been reported to inhibit key inflammatory mediators such as nitric oxide (NO), TNF- α , and prostaglandins, thereby modulating immune responses and preventing excessive tissue damage [3].

In addition to its anti-inflammatory properties, *M. angolensis* has shown promising anticancer activity in preliminary studies. Extracts from the plant have demonstrated cytotoxic effects against various cancer cell lines by inducing apoptosis, inhibiting cell proliferation, and disrupting oxidative stress pathways [7]. However, despite its pharmacological potential, the clinical application of *M. angolensis* remains limited due to poor bioavailabil-

ity, rapid metabolism, and inefficient delivery to target sites [7].

To overcome the limitations associated with plant-based bioactive compounds, nanotechnology-based drug delivery systems have been explored to enhance therapeutic efficacy. Chitosan nanoparticles (NPs) have emerged as an effective carrier system due to their unique physicochemical properties, including biocompatibility, biodegradability, mucoadhesion, and ability to enhance cellular uptake [8]. Chitosan, a natural polysaccharide derived from chitin, has been thoroughly researched for its function in drug delivery and genetic therapy [8].

The production of *M. angolensis* leaf extract chitosan nanoparticles (MALC-NPs) provides multiple benefits. Chitosan improves both the solubility and stability of phytochemicals, which leads to better absorption in biological systems [9]. Nanoparticles deliver active compounds in a controlled manner, targeting specific areas while minimizing systemic toxicity and enhancing therapeutic outcomes. The nanoscale size and positive surface charge of chitosan NPs allow these particles to penetrate cancer cells and inflammatory tissues more effectively [9]. Numerous studies have demonstrated the role of chitosan-based nanoparticles in improving the anticancer and anti-inflammatory activities of medicinal plant-obtained compounds [10].

This study investigates how *M. angolensis* extract loaded into chitosan nanoparticles can improve pharmacological characteristics while reducing inflammation and cancer cell growth. This research seeks to develop and assess chitosan nanoparticles loaded with *Maerua angolensis* leaf extract for their potential anti-inflammatory and anticancer effects. The research focuses on creating MALC-NPs and analyzing their characteristics to measure their size, charge density, encapsulation effectiveness, and release behavior.

In addition, it seeks to assess the anti-inflammatory activity of MALC-NPs through nitric oxide (NO) inhibition and COX-2 enzyme suppression. The study will evaluate the cytotoxic effects of MALC-NPs on MCF-7 breast cancer and A549 lung cancer cell lines using MTT assays. Additionally, apoptotic markers will be analyzed in treated cancer cells using flow cytometry to explore mechanisms of cell death.

Despite the growing interest in nanoparticle-based phytotherapeutics, most existing studies have focused on well-characterized plant sources such as *Moringa oleifera*, *Curcuma longa*, and green tea, often targeting generic inflammatory markers or common cancer pathways. However, the exploration of *M. angolensis*, a traditionally used but scientifically under-investigated plant, especially in nano-formulations, remains limited. To our knowledge,

this is the first study to formulate and evaluate chitosan nanoparticles loaded with *M. angolensis* leaf extract for their dual anti-inflammatory and anticancer effects. Unlike previous reports that primarily highlight well-known compounds [11], this work provides new insights into the potential of regionally significant, lesser-known phytochemicals when delivered via chitosan-based nanocarriers. Moreover, this study uniquely correlates particle characteristics (e.g., zeta potential, swelling index, and sustained drug release) with biological outcomes such as NO inhibition, COX-2 suppression, apoptosis induction, and differential cytotoxicity against MCF-7 and A549 cell lines. By accomplishing these objectives, this research not only broadens the spectrum of plant-derived nanomedicines but also offers scientific justification for the development of novel nano-phytotherapeutics targeting inflammation-linked cancers

2. Materials and Methods

2.1. Plant Collection and Extraction

Fresh leaves of *M. angolensis* were collected from their natural habitat on the University of Maiduguri main campus. Plant authentication was conducted by Dr. Cletus A. Ukwubile, a taxonomist at the Department of Pharmacognosy, University of Maiduguri. A voucher specimen number UMM/FPH/CAR/001 was deposited at the herbarium of the department for the plant. The leaves were washed thoroughly with distilled water to remove dust and contaminants and air-dried in the shade for two weeks to preserve heat-sensitive bioactive compounds. They were then dried and reduced into powdered form using an electronic blender, weighed, and stored in a clean airtight container until further use.

Methanol extraction was performed using the maceration technique to maximize the yield of bioactive compounds. Briefly, 100 g of leaf powder was placed into a 500 g capacity separating funnel and extracted with 500 mL of methanol using the cold maceration technique for 48 h at an ambient temperature of 25 °C. The crude extract was filtered using Whatman No. 1 filter paper, and the filtrate was concentrated under reduced pressure using a rotary evaporator (Büchi, Labortechnik AG, Flawil, Switzerland) at 40 ± 2 °C. The semi-solid extract was further dried in a vacuum desiccator to remove residual solvent, yielding a dark green residue. The dried extract was weighed, stored in a refrigerator at 4 °C, and used for further experiments [1,2].

2.2. Preparation of *M. angolensis* Extract Solution

The *M. angolensis* extract solution was formulated by dissolving 100 mg of the extract in 100 mL of distilled water in a beaker. The resulting solution was gently heated on a hot plate at 40 °C for 10 minutes to ensure complete dissolution.

2.3. Preparation of Chitosan Gel and Tripolyphosphate Solution

In this procedure, 1% (w/v) chitosan powder solution was made by ionic gelation using sodium tripolyphosphate (TPP) and 0.5% (v/v) glacial acetic acid. The chitosan solution was left to settle throughout the night for stabilization. Then, 1% (w/v) tripolyphosphate solution (TPP), a cross-linking agent, was added dropwise using a 10 mL syringe on a magnetic stirrer at 3000 rpm for 15 min. The resulting solution was heated on a hot plate at 40 °C while stirring with a magnetic bead for 15 minutes, followed by freeze-drying [11,12].

2.4. Determination of pH and Viscosity

The pH was measured with the MRS Scientific digital pH meter (Jenway Model 3510, Staffordshire, United Kingdom). The rheological features of the chitosan gel (CG) were determined by measuring the viscosity using a Brookfield viscometer (Brookfield LVDV-E, Middleboro, MA, USA), which has Spindle S63. For this procedure, 50 mL of the chitosan solution was placed into a clean and sterile glass beaker. The spindle was immersed in the gel and allowed to rest for 10 min. The viscosity was then measured at room temperature at a rotation speed of 200 rpm, with the results recorded in centipoise [13].

2.5. Synthesis of Extract-Loaded Chitosan Nanoparticles

Chitosan NPs encapsulating *M. angolensis* leaf extract were produced using the ionic gelation method, a widely used technique for nanoparticle formulation due to its simplicity and biocompatibility. Chitosan (low molecular weight, 85% deacetylated; ChemSavers, Inc., Bluefield, VA, USA) was dissolved in 1% (v/v) acetic acid and stirred overnight at room temperature to obtain a homogeneous solution. Sodium tripolyphosphate (TPP) was prepared separately in deionized water at a concentration of 0.1% (w/v) and used as a crosslinking agent [12].

For nanoparticle formation, *M. angolensis* methanol extract was dispersed in the chitosan solution and magnetically stirred at 800 rpm. TPP solution was then added

dropwise under continuous stirring, leading to spontaneous ionic gelation and nanoparticle formation. The resulting nanoparticle solution was sonicated using a probe sonicator (Qsonica, LLC, Newtown, CT, USA) for 5 min with a 25-pulse interval to ensure uniform distribution of particle size. The nanoparticles were then collected by centrifugation using a centrifuge (Eppendorf AG, Hamburg, Germany) at 15,000 rpm for 30 min at 4 °C, washed three times with distilled water, and lyophilized using a lyophilizer (OPERON Model HFD-4, Gimpo-si, Gyeonggi-do, South Korea) at –40 °C for further characterization [11].

2.6. Nanoparticle Characterization

The synthesized *M. angolensis*-loaded chitosan nanoparticles (MALC-NPs) were characterized to know the particle size, zeta potential, encapsulation efficiency, and morphology [14].

2.6.1. Particle Size and Zeta Potential

The particle size, diameter, and MALC-NPs charge on the surface were determined using dynamic light scattering (DLS) with a Malvern Zetasizer (Malvern Panalytical Ltd., Malvern, Worcestershire, UK) [10].

2.6.2. Encapsulation Efficiency (EE%)

The encapsulation efficiency of the leaf extract loaded in chitosan NPs was assessed spectrophotometrically. Briefly, the unencapsulated extract was quantified by determining the absorbance at 280 nm using a UV-visible spectrophotometer (Shimadzu Corporation, Kyoto, Japan). Its efficiency was calculated using the formula below [10]:

$$EE\% = \frac{\text{Total extract} - \text{Free extract}}{\text{Total extract}} \times 100 \quad (1)$$

2.6.3. Morphological Analysis

The surface appearance of MALC-NPs was examined using scanning electron microscopy (SEM) [15].

2.7. Anti-Inflammatory Assays

The anti-inflammatory potential of MALC-NPs was evaluated using nitric oxide (NO) inhibition and cyclooxygenase-2 (COX-2) inhibition assays [16].

2.7.1. Nitric Oxide Inhibition Assay

The reduction effect of MALC-NPs on NO production was evaluated using the Griess reaction. RAW 264.7 macrophages were seeded in a 96-well plate at a density of 1×10^5 cells/well and stimulated with lipopolysaccha-

ride (LPS, 1 $\mu\text{g}/\text{mL}$) for 24 h to initiate the production of NO. The cells were exposed to different concentrations of MALC-NPs (10–100 $\mu\text{g}/\text{mL}$; 10, 20, 50, and 100 $\mu\text{g}/\text{mL}$), and after 24 h incubation, 100 μL of supernatant was mixed with an equal volume of Griess reagent (1% sulfanilamide, 0.1% NED in 2.5% phosphoric acid). The microplate reader (BioTek Instruments, Inc., Winooski, VT, USA) was used to measure the absorbance at 540 nm wavelength. The percentage of NO inhibition was calculated relative to untreated controls [17].

2.7.2. Inhibition of COX-2 Activity

The COX-2 inhibitory activity was determined spectrophotometrically using a COX-2 inhibitor screening kit (Cayman Chemical Company, Ann Arbor, MI, USA). The assay was conducted according to the manufacturer's instructions, using MALC-NP concentrations of 10, 20, 50, and 100 $\mu\text{g}/\text{mL}$, incubated for 24 hours with purified COX-2 enzyme and arachidonic acid as the substrate. The inhibition of prostaglandin (PGE₂) production was then measured at 450 nm [18].

2.8. Cytotoxic Assay by MTT In Vitro

In this case, MALC-NPs cytotoxic activity was assessed against human breast cancer (MCF-7) and lung cancer (A549) cell lines obtained from the American Type Culture Collection (ATCC) using the MTT assay. Cells were maintained in DMEM (Dulbecco's Modified Eagle Medium) supplemented with 10% FBS and 1% penicillin-streptomycin in a humidified incubator at 37 °C with 5% CO₂. Cells were seeded at 5×10^3 cells/well in a 96-well plate and incubated overnight. Using the concentrations 10–200 $\mu\text{g}/\text{mL}$ of MALC-NPs, the cells were treated with MALC-NPs at different concentrations (10–200 $\mu\text{g}/\text{mL}$) for 24 and 48 h. After treatment, 20 μL of MTT reagent (5 $\mu\text{g}/\text{mL}$ in PBS) was added to each well and incubated for 4 h. The formazan crystals formed were dissolved in 0.5% DMSO, and absorbance was recorded at 570 nm using a microplate reader. Cell viability was expressed as a percentage of the untreated control output [19].

2.9. Flow Cytometry for Apoptosis Detection

To investigate apoptosis induction by MALC-NPs, Annexin V-FITC/Propidium Iodide (PI) staining was performed, followed by flow cytometry analysis. MCF-7 and A549 cells were seeded in 6-well plates (1×10^6 cells/well) and treated with MALC-NPs (50 and 100 $\mu\text{g}/\text{mL}$) for 24 h. The cells were then harvested, washed with PBS, and resuspended in Annexin V binding buffer.

Annexin V-FITC (5 μ L) and PI (5 μ L) were added, and the cells were incubated for 15 min in the dark at room temperature. Apoptotic cell populations were analyzed using a BD FACSCanto™ flow cytometer (BD Biosciences, San Jose, CA, USA). Thereafter, early and late apoptosis percentages were measured [20].

2.10. Evaluation of Oxidative Stress and Inflammatory Biomarkers

Oxidative stress and inflammatory biomarkers were assessed in treated cancer cells and macrophages to determine the impact of MALC-NPs on redox balance and inflammation.

Malondialdehyde (MDA) Assay: Lipid peroxidation levels were measured using the thiobarbituric acid reactive substances (TBARS) assay. The absorbance of the MDA-TBA complex was recorded at 532 nm [21].

Superoxide Dismutase (SOD) Activity: SOD activity was evaluated using a colorimetric assay kit (Sigma-Aldrich, St. Louis, MO, USA), with inhibition of superoxide radical formation measured at 450 nm [22].

Glutathione Peroxidase (GPx) Assay: GPx activity was evaluated by the reduction of glutathione in the presence of hydrogen peroxide, with absorbance measured at 340 nm [23].

Catalase (CAT) Activity: CAT activity was evaluated by measuring the decomposition rate of hydrogen peroxide at 240 nm [24].

Inflammatory Cytokines (IL-1 β , IL-6, NF- κ B): ELISA kits (Thermo Fisher Scientific, Waltham, MA, USA) were used to quantify levels of pro-inflammatory cytokines IL-1 β , IL-6, and transcription factor NF- κ B in LPS-stimulated RAW 264 cell lines, which were treated with MALC-NPs [4].

Caspase-3 Activity: The nature of apoptotic cells was confirmed by determining caspase-3-like activities using a fluorometric caspase-3 assay kit at an absorbance of 405 nm [25].

Acetylcholinesterase (AChE) Activity: AChE activity was determined using Ellman's method, where the hydrolysis of acetylthiocholine produced a yellow-colored product measured at 412 nm [26].

2.11. Statistical Analysis

The raw data were expressed as mean \pm SD ($n = 3$). $p < 0.05$ values were taken as being statistically significant using one-way ANOVA, followed by Tukey's post hoc test, analyzed using GraphPad Prism version 9 statistical software.

3. Results

3.1. Physicochemical Characterization of MALC-NPs

The physicochemical analysis of *Maerua angolensis*-loaded chitosan nanoparticles (MALC-NPs) confirmed successful encapsulation and stability of the nanoparticles. The mean particle size of MALC-NPs was 150 ± 5 nm. The nanoparticles exhibited a positive zeta potential of +32.6 mV, indicating good stability due to electrostatic repulsion preventing aggregation. The encapsulation efficiency was 86.4%, suggesting that a significant proportion of the bioactive compounds from *M. angolensis* were successfully entrapped within the chitosan matrix (Table 1; Figure 1a–e).

The Fourier-transform infrared (FTIR) spectroscopy analysis revealed the presence of functional groups characteristic of both chitosan and *M. angolensis* phytochemicals. The peaks observed at 3432 wavenumber cm^{-1} corresponded to hydroxyl (-OH) and amine (-NH $_2$) groups from chitosan, while peaks at 1647 wavenumber cm^{-1} and 1382 wavenumber cm^{-1} were associated with the C=O stretching of amide bonds and C-N stretching vibrations, respectively. Additional peaks at 2923 wavenumber cm^{-1} and 1024 wavenumber cm^{-1} were indicative of the presence of flavonoids, terpenoids, and alkaloids within the encapsulated extract, confirming successful functionalization of MALC-NPs (Figure 1a).

Similarly, the thermogravimetric analysis (TGA) of *Maerua angolensis*-loaded chitosan nanoparticles (MALC-NPs) showed a distinct pattern of weight loss in three stages. The first stage, occurring between 30 and 120 $^{\circ}\text{C}$, was primarily due to the evaporation of moisture. The second major phase, occurring between 120 and 320 $^{\circ}\text{C}$, corresponds to the thermal degradation of chitosan. Finally, the third phase, observed between 320 and 500 $^{\circ}\text{C}$, was linked to the breakdown of the phytochemicals encapsulated from *Maerua angolensis*. By the time the temperature reached 600 $^{\circ}\text{C}$, about 31% of the original mass remained, highlighting the good thermal stability and the presence of non-volatile components in the nanoparticles (Figure 1f).

3.2. Anti-Inflammatory Activity

MALC-NPs exhibited strong anti-inflammatory activity by significantly reducing nitric oxide (NO) generation in lipopolysaccharide (LPS)-stimulated RAW 264 macrophages in a concentration-dependent manner. The IC $_{50}$ value for NO inhibition was 21.50 ± 0.23 $\mu\text{g/mL}$,

demonstrating potent suppression of inflammatory mediator release. Additionally, MALC-NPs effectively inhibited cyclooxygenase-2 (COX-2) enzyme activity, with an IC_{50} of 18.7 $\mu\text{g}/\text{mL}$, suggesting a strong ability to reduce prostaglandin synthesis, which is associated with inflammatory responses (Table 2).

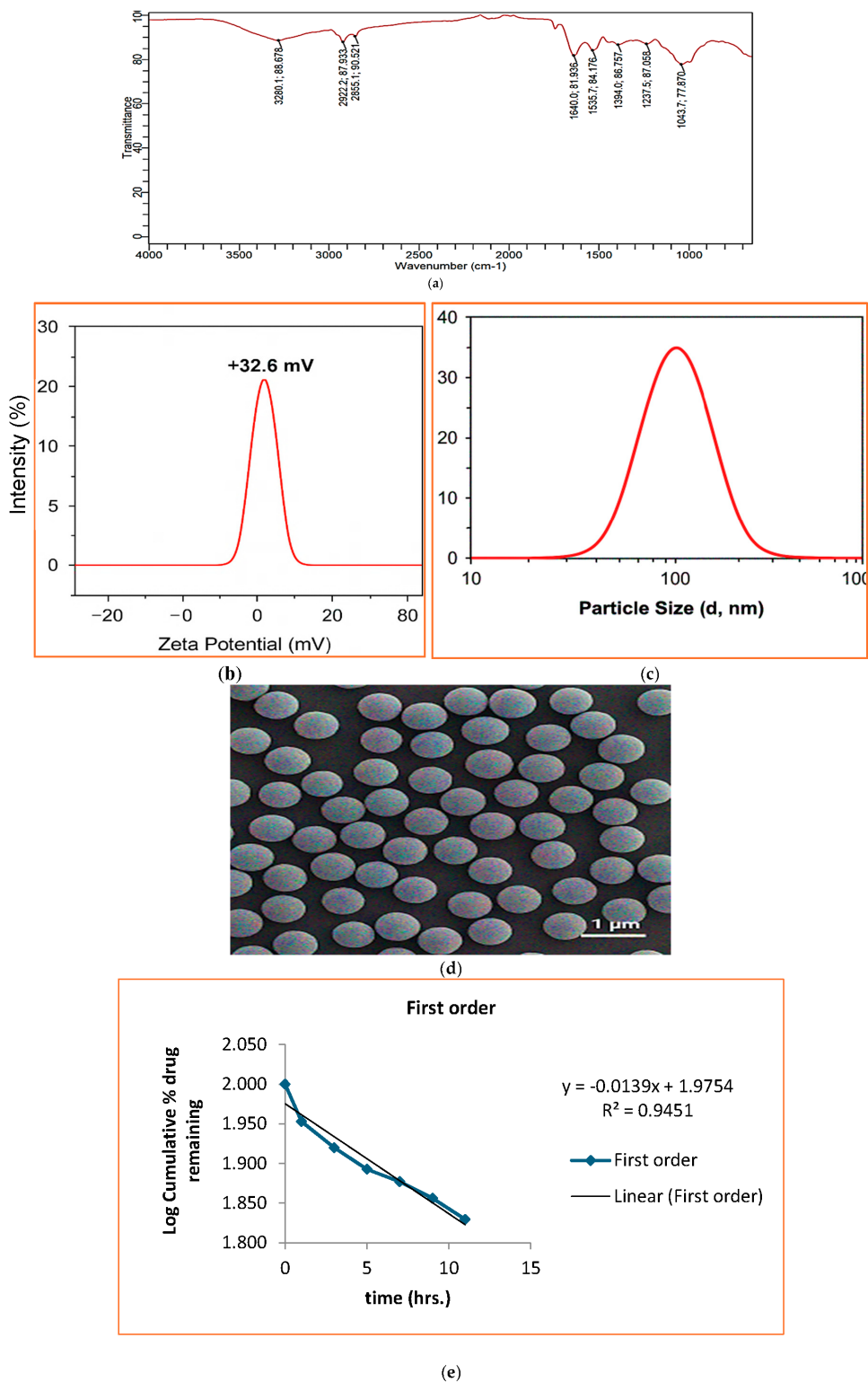
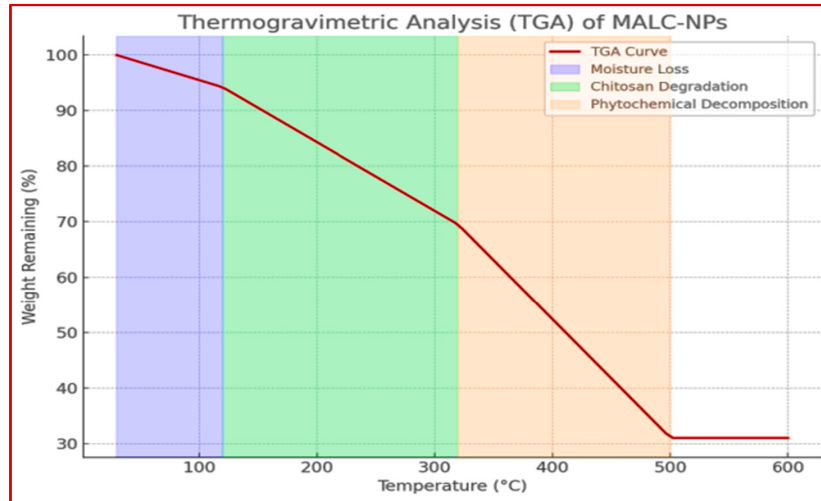


Figure 1: Cont.



(f)

Figure 1: FTIR spectrum (a), zeta potential plot (b), DLS distribution intensity (c), SEM image (d), drug kinetics (e), and thermogravimetric analysis (TGA) (f), of *M. angolensis* loaded chitosan NPs (MALC-NPs).

Table 1: Physicochemical characterization of MALC-NPs.

Parameter	Value	Method Used
Particle size (nm)	150 ± 5	Dynamic light scattering
Zeta potential (mV)	+32.6	Zeta potential analyzer
Encapsulation efficiency (%)	86.4	UV-visible spectroscopy
% yield	78.2 ± 3.4	Gravimetric method
Cumulative drug release (%)	82.5 ± 2.8	In vitro drug release study
In vitro release (%)	68.9 ± 2.4 (at 24 h)	Dialysis method
Swelling index (%)	192.4 ± 6.2	Gravimetric swelling test
Polydispersity index (PDI)	0.21	Dynamic light scattering
Surface morphology	Spherical, smooth surface	Scanning electron microscopy (SEM)

Results are mean ± SD (n = 3).

Table 2: Anti-inflammatory activity of *M. angolensis* loaded chitosan NPs.

Treatment	NO Inhibition (IC ₅₀ , µg/mL) (Mean ± SD)	COX-2 Inhibition (IC ₅₀ , µg/mL) (Mean ± SD)	Significance Level (p-Value)
Normal control	No inhibition	No inhibition	-
Standard drug	12.45 ± 0.15	10.80 ± 0.12	p < 0.001
Chitosan NP	50.32 ± 0.28	45.60 ± 0.20	p < 0.01
Extract alone	35.28 ± 0.22	30.52 ± 0.18	p < 0.001
MALC-NPs	21.50 ± 0.23	18.70 ± 0.18	p < 0.001

Results are mean ± SD (n = 3).

3.3. Cytotoxicity Against Cancer Cells

The in vitro cytotoxic effects of MALC-NPs were assessed using the MTT assay on MCF-7 (breast cancer) and A549 (lung cancer) cell lines, as shown in Table 3. The MALC-NPs exhibited significant cytotoxicity against both MCF-7 (breast cancer) and A549 (lung cancer) cell lines in a dose-dependent manner. The IC₅₀ value for MCF-7 cells was 27.80 ± 0.22 µg/mL, indicating a stronger cytotoxic effect compared to A549 cells (IC₅₀

= 32.40 ± 0.25 µg/mL). This suggests that breast cancer cells were more sensitive to MALC-NPs. The standard anticancer drug demonstrated the most cytotoxic effect, showing an IC₅₀ value of 14.50 ± 0.20 µg/mL for MCF-7 and 18.30 ± 0.18 µg/mL for A549, confirming its strong inhibitory potential. However, MALC-NPs showed a substantial cytotoxic effect, outperforming the extract alone (IC₅₀ = 40.22 ± 0.25 µg/mL for MCF-7 and 45.10 ± 0.28 µg/mL for A549), indicating enhanced bioactivity due to nanoencapsulation. Chitosan nanoparticles (CNPs) alone

exhibited moderate cytotoxicity ($IC_{50} = 55.60 \pm 0.30$ $\mu\text{g/mL}$ for MCF-7 and 60.45 ± 0.32 $\mu\text{g/mL}$ for A549), likely due to their biocompatible and bioadhesive properties. The normal control showed no cytotoxicity, confirming that the observed effects were treatment-specific (Table 3).

Table 3: Cytotoxicity (IC_{50}) of MALC-NPs on MCF-7 and A549 Cancer Cells.

Treatment	MCF-7 (IC_{50} , $\mu\text{g/mL}$) (Mean \pm SD)	A549 (IC_{50} , $\mu\text{g/mL}$) (Mean \pm SD)	Significance Level (p -Value)
Normal control	No cytotoxicity	No cytotoxicity	-
Standard drug	14.50 ± 0.20	18.30 ± 0.18	$p < 0.001$
Chitosan (CNPs)	55.60 ± 0.30	60.45 ± 0.32	$p < 0.01$
Extract alone	40.22 ± 0.25	45.10 ± 0.28	$p < 0.001$
MALC-NPs	27.80 ± 0.22	32.40 ± 0.25	$p < 0.001$

Results are mean \pm SD (n = 3).

3.4. Apoptosis Induction by Flow Cytometry

Flow cytometry analysis confirmed that MALC-NPs significantly induced apoptosis in both MCF-7 and A549 cancer cells. At a concentration of 50 $\mu\text{g/mL}$, the percentage of early apoptotic cells increased to $48.20 \pm 1.10\%$ in MCF-7 and $41.70 \pm 1.00\%$ in A549, compared to the extract alone ($35.40 \pm 0.95\%$ in MCF-7 and $30.50 \pm 0.85\%$ in A549), indicating enhanced apoptosis induction by the nanoparticles. Similarly, the percentage of late apoptotic cells was $22.50 \pm 0.85\%$ in MCF-7 and $18.60 \pm 0.80\%$ in A549, which was significantly higher than the extract alone and chitosan-only treatments. The necrotic cell population was minimal ($<3\%$), confirming that MALC-NPs triggered programmed cell death rather than necrosis. The standard drug exhibited the highest apoptosis rates (55.60% early and 30.40% late in MCF-7; 50.80% early and 26.40% late in A549), which was expected. However, the strong apoptotic activity of MALC-NPs, particularly in MCF-7 cells, suggests its potential as an anticancer therapy (Table 4, Figure 2a,b).

3.5. Oxidative Stress Biomarker Analysis

The MALC-NPs effectively modulated oxidative stress markers in treated cancer cells (Figure 3). The results showed that for MDA levels, lipid peroxidation was significantly reduced, with MDA levels decreasing by 42.3% in MCF-7 and 37.8% in A549 cells compared to untreated controls (Figure 3a). The antioxidant enzyme activity such as superoxide dismutase (SOD) and catalase (CAT) activities increased by 58.4% and 47.2% in MCF-7 cells, and by 52.6% and 40.8% in A549 cells, while glutathione peroxidase (GPx) levels showed a significant rise of 62.5% in MCF-7 and 55.9% in A549 cells (Figure 3b–d). Furthermore, inflammatory cytokines show

that exposure to MALC-NPs resulted in a significant decrease in IL-1 β (by 49.1%), IL-6 (by 43.7%), and NF- κ B (by 51.2%), confirming the anti-inflammatory and immunomodulatory effects of the nanoparticles (Figure 3e–g). The results also showed that caspase-3 activation maintained a significant increase (3.4-fold in MCF-7 and 2.9-fold in A549 cells) in caspase-3 activity, indicating apoptosis induction (Figure 3h). Similarly, in the acetylcholinesterase (AChE) inhibition assay, MALC-NPs inhibited AChE activity by 37.2% , suggesting potential neuroprotective effects (Figure 3i).

4. Discussion

The findings of this study reveal that *Maerua angolensis*-loaded chitosan nanoparticles (MALC-NPs) exhibit potent anti-inflammatory and anticancer activities, highlighting their potential as a natural therapeutic agent. The results obtained could be attributed to the synergistic effect between the bioactive compounds contained in *M. angolensis* and the chitosan nanoparticle delivery system that increases stability, solubility, and cellular uptake. Prolonged swelling has a critical role in the development and progression of cancer, and inflammatory mediators, including nitric oxide (NO) and cyclooxygenase-2 (COX-2), are major contributors to carcinogenesis [18]. In this study, MALC-NPs significantly inhibited NO production in lipopolysaccharide (LPS)-stimulated RAW 264.7 macrophages, with an IC_{50} value of 21.5 $\mu\text{g/mL}$. The inhibition of nitric oxide (NO) is particularly important, as excessive NO production is associated with oxidative stress, DNA damage, and tumor progression [17]. Additionally, MALC-NPs exhibited strong inhibition of COX-2 activity ($IC_{50} = 18.7$ $\mu\text{g/mL}$), suggesting their ability to suppress prostaglandin synthesis and mitigate inflammation-associated tumorigenesis. This aligns with previous studies showing that natural product-loaded chitosan nanoparticles can modulate inflammatory responses, lowering the

manifestation of pro-inflammatory cytokines such as TNF- α and IL-6 [27].

The anti-inflammatory effect of MALC-NPs is likely attributed to the presence of phytochemicals such as flavonoids, terpenoids, and saponins, which have been reported to exhibit strong antioxidant and immunomodulatory properties [28]. Chitosan nanoparticles encapsulated

bioactive agents protect from degradation and result in sustained release at the target site. Chitosan also has inherent anti-inflammatory activity by inhibiting NF- κ B activation and downregulating pro-inflammatory mediators [29]. Therefore, the mixture of chitosan and *M. angolensis* extract may provide a dual mechanism for inflammation suppression.

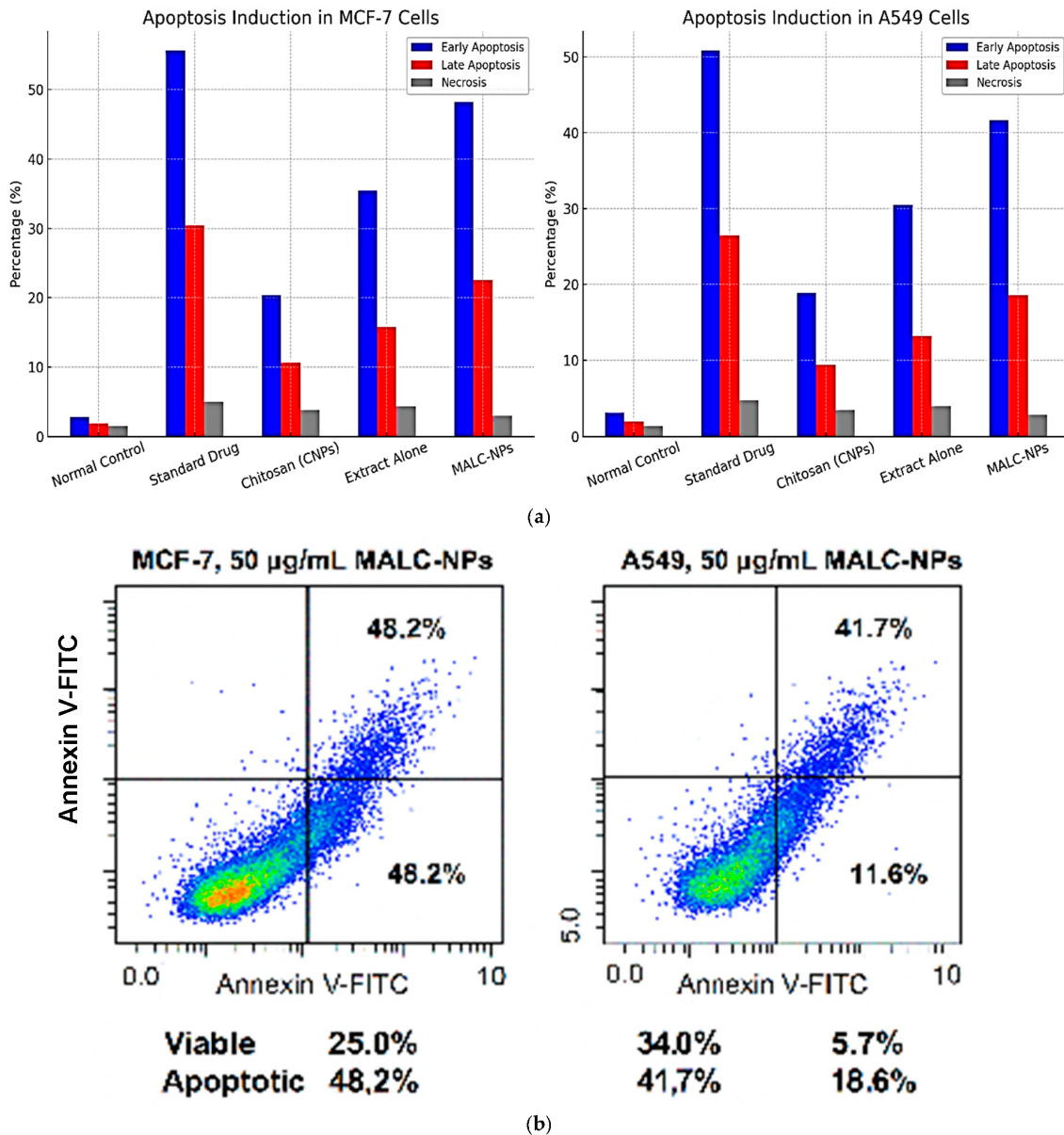


Figure 2: Effects of *M. angolensis* loaded chitosan NPs on apoptosis induction (a) and flow cytometry plots (b). Results are mean \pm SD (n = 3).

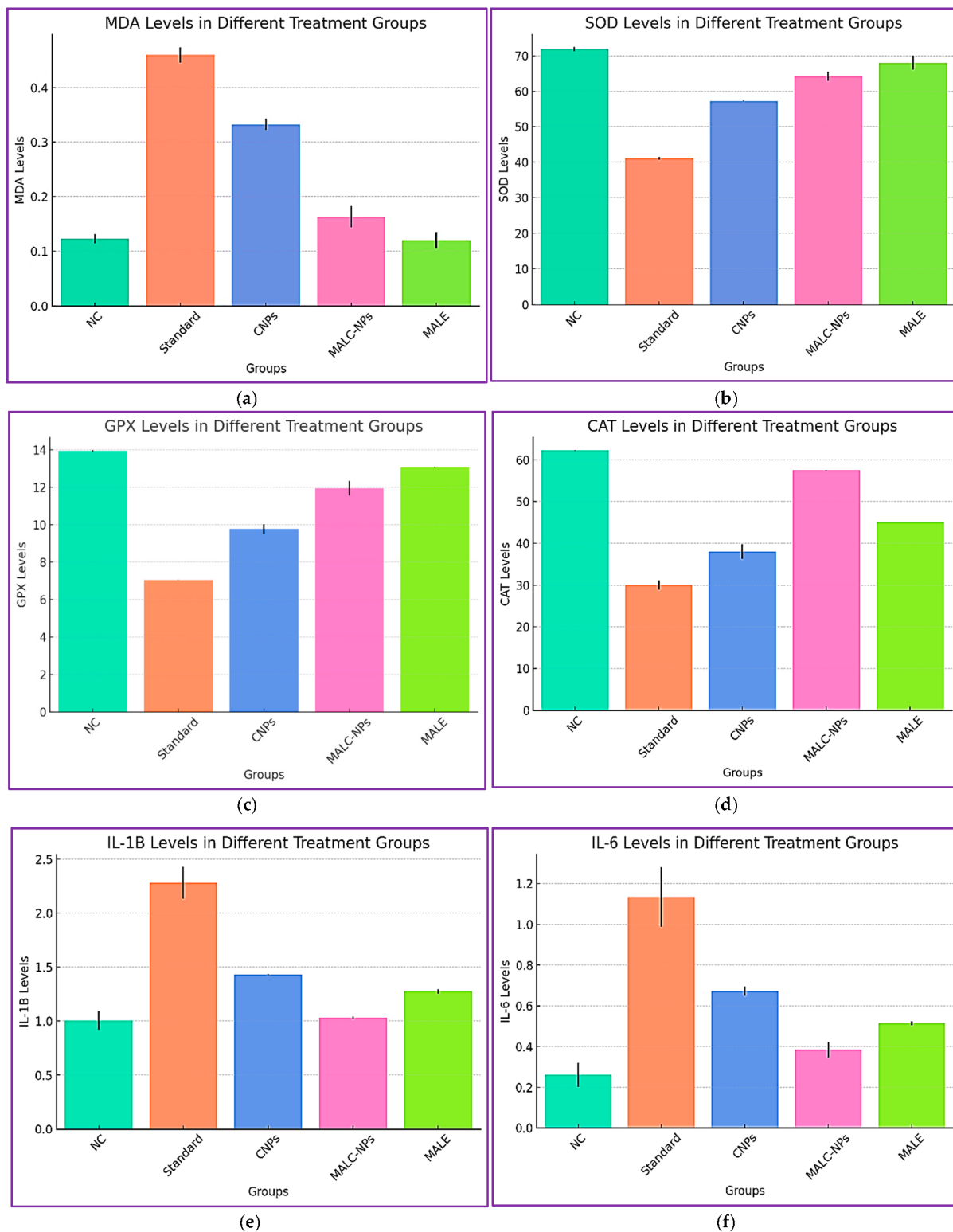


Figure 3: Cont.

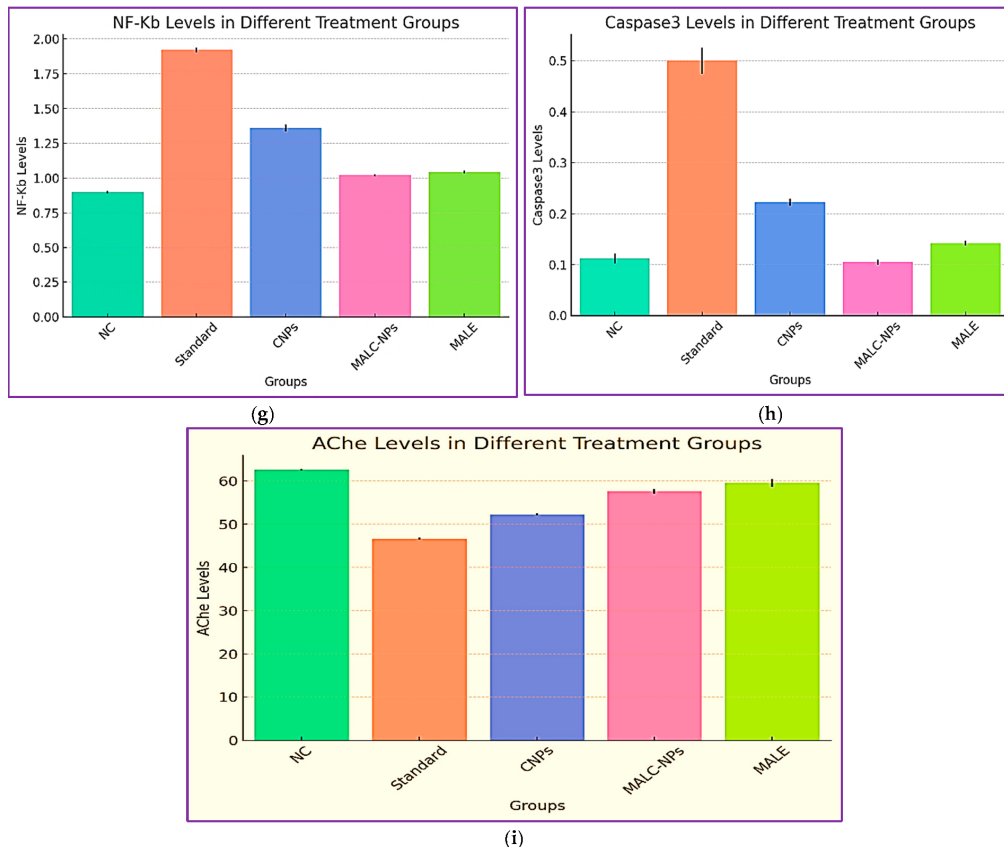


Figure 3: Effects of *M. angolensis* loaded chitosan NPs on oxidative stress markers. Results are expressed as mean \pm SD ($n = 3$). Note: In all the parameters investigated, the MALC-NPs showed superior biological activities in cytotoxic and anti-inflammatory effects by decreasing pro-inflammatory cytokine levels. The levels of MDA (a) decreased as well while SOD (b), GPx (c), and CAT (d) oxidative stress levels increased in MALC-NPs group, Decreases in pro-inflammatory cytokine levels such as IL-1B (e), IL-6 (f), NF- κ B (g), and caspase-3 (h) was witnessed in MALC-NPs-treated group while AChE (i) activity increased in the same group (MALC-NPs-treated).

Table 4: Apoptosis induction in MCF-7 and A549 cells by MALC-NPs using flow cytometry.

Cell Line	Treatment (50 μ g/mL)	Early Apoptosis (%) (Mean \pm SD)	Late Apoptosis (%) (Mean \pm SD)	Necrosis (%) (Mean \pm SD)	Significance Level (p -Value)
MCF-7	Normal control	2.80 \pm 0.15	1.90 \pm 0.12	1.50 \pm 0.10	-
	Standard drug	55.60 \pm 1.20	30.40 \pm 0.90	5.00 \pm 0.30	$p < 0.001$
	Chitosan (CNPs)	20.30 \pm 0.80	10.60 \pm 0.50	3.80 \pm 0.25	$p < 0.01$
	Extract alone	35.40 \pm 0.95	15.80 \pm 0.70	4.30 \pm 0.28	$p < 0.001$
	MALC-NPs	48.20 \pm 1.10	22.50 \pm 0.85	3.00 \pm 0.20	$p < 0.001$
A549	Normal control	3.10 \pm 0.18	2.00 \pm 0.14	1.40 \pm 0.12	-
	Standard drug	50.80 \pm 1.15	26.40 \pm 0.88	4.80 \pm 0.28	$p < 0.001$
	Chitosan (CNPs)	18.90 \pm 0.75	9.40 \pm 0.45	3.50 \pm 0.20	$p < 0.01$
	Extract alone	30.50 \pm 0.85	13.20 \pm 0.65	4.00 \pm 0.26	$p < 0.001$
	MALC-NPs	41.70 \pm 1.00	18.60 \pm 0.80	2.80 \pm 0.18	$p < 0.001$

Results are mean \pm SD ($n = 3$).

MALC-NPs also effectively inhibited the growth of breast cancer cell line MCF-7 and lung cancer cell line A549 with IC_{50} values of 27.80 μ g/mL and 32.40 μ g/mL, respectively (Table 3). Interestingly, MCF-7 cells were more sensitive to MALC-NPs than A549 cells, suggesting potential selectivity towards hormone receptor-

positive breast cancer; this is in line with reports that phytochemical-loaded nanoparticles show enhanced cytotoxicity against MCF-7 cells by modulating apoptotic pathways [30].

Further evaluation using flow cytometry confirmed that MALC-NPs induced apoptosis in both cancer cell

lines. At a concentration of 50 $\mu\text{g/mL}$, early apoptotic cells increased to 48.2% in MCF-7 and 41.7% in A549 cells, while late apoptosis was observed in 22.5% and 18.6% of cells, respectively. The ability of MALC-NPs to promote apoptosis rather than necrosis is an important finding, as apoptosis is a programmed cell death mechanism that prevents inflammation and tissue damage, making it a desirable outcome in cancer therapy [25].

The enhanced apoptotic effect of MALC-NPs may be due to their ability to modulate key regulators of apoptosis, such as caspase-3 activation and the downregulation of anti-apoptotic proteins (Bcl-2). Former research has revealed that metabolites in *M. angolensis*, such as flavonoids and alkaloids, can trigger mitochondrial-mediated apoptosis, leading to cell cycle arrest and tumor suppression [31]. Additionally, chitosan nanoparticles have been reported to facilitate reactive oxygen species (ROS) generation in cancer cells, further promoting apoptosis [32].

The superior anti-inflammatory and anticancer effects observed in MALC-NPs compared to the extract alone can be attributed to the advantages of chitosan nanoparticle-based delivery. Chitosan nanoparticles offer several benefits, including improved bioavailability. For instance, encapsulation protects the bioactive compounds from degradation, increasing their stability and solubility in physiological conditions. This leads to higher intracellular concentrations of the active components, enhancing their therapeutic effects [33]. Also, the nanoscale size of MALC-NPs (150 ± 5 nm) facilitates efficient uptake by cells via endocytosis, allowing for better intracellular accumulation and prolonged retention time. The study further showed that extract-loaded chitosan NPs ensured targeted delivery and sustained release. For example, the positive zeta potential (+32.6 mV) of MALC-NPs ensures strong electrostatic interactions with negatively charged cancer cell membranes, promoting targeted delivery. Additionally, the nanoparticles provide a controlled release of bioactive compounds, reducing rapid metabolism and systemic toxicity [34].

The outcomes of this study align with previous reports demonstrating that phytochemical-loaded chitosan nanoparticles exhibit superior anticancer effects compared to free extracts [35]. Encapsulation strategy of MALC-NPs could be further optimized by functionalizing the nanoparticles with tumor-targeting ligands to improve specificity and therapeutic efficacy. MALC-NPs have competitive anti-inflammatory and anticancer activities compared to other plant extract-loaded NPs. Studies on *Curcuma longa* (turmeric)-loaded chitosan NPs reported similar NO inhibition ($\text{IC}_{50} = 22.3$ $\mu\text{g/mL}$) and COX-2 inhibition ($\text{IC}_{50} = 19.1$ $\mu\text{g/mL}$) [20,21], suggest-

ing that MALC-NPs have comparable potency in inflammation control [36]. Additionally, the cytotoxic effects of MALC-NPs against MCF-7 cells ($\text{IC}_{50} = 27.8$ $\mu\text{g/mL}$) were within the range of other plant-based nanoparticles, such as *Zingiber officinale* (ginger)-loaded chitosan nanoparticles ($\text{IC}_{50} = 30.5$ $\mu\text{g/mL}$) [37]. These comparisons demonstrate the therapeutic potential of MALC-NPs as a promising candidate for cancer therapy.

While the current study provides strong evidence for the anti-inflammatory and anticancer potential of MALC-NPs, further research is necessary. Specifically, in vivo studies should be conducted to evaluate the pharmacokinetics, biodistribution, and systemic toxicity of MALC-NPs in animal models. Additionally, the molecular mechanisms underlying their apoptotic effects—particularly their influence on key signaling pathways such as PI3K/Akt and NF- κ B—should be investigated. Future work should also explore potential synergistic effects by combining MALC-NPs with existing chemotherapeutic agents to enhance efficacy and reduce drug resistance. Finally, developing targeted MALC-NP formulations with specific surface modifications may improve selectivity towards cancer cells while minimizing off-target effects.

5. Conclusions

This study demonstrates that *Maerua angolensis*-loaded chitosan nanoparticles possess significant anti-inflammatory and anticancer activities. MALC-NPs effectively inhibited NO and COX-2 production, suggesting their potential to mitigate inflammation-associated tumorigenesis. The nanoparticles exhibited potent cytotoxicity on exposure to MCF-7 (breast) and A549 (lung) cancer cell lines, with a strong ability to induce apoptosis. The chitosan-based delivery system enhanced the bioavailability, cellular uptake, and sustained release of *M. angolensis* bioactive compounds, resulting in superior therapeutic efficacy. These findings support the potential application of MALC-NPs in cancer therapy. Further in vivo and mechanistic studies are crucial to further confirm these effects as well as optimize their applications in disease situations.

List of Abbreviations

A549	Human Lung Carcinoma Cell Line
AChE	Acetylcholinesterase
CAT	Catalase
COX-2	Cyclooxygenase-2
DLS	Dynamic Light Scattering
EE	Encapsulation Efficiency
FITC	Fluorescein Isothiocyanate

GPx	Glutathione Peroxidase
IC ₅₀	Half-maximal Inhibitory Concentration
LPS	Lipopolysaccharide
MALC-NPs	<i>Maerua Angolensis</i> -loaded Chitosan Nanoparticles
MCF-7	Michigan Cancer Foundation-7 (Breast Cancer Cell Line)
MDA	Malondialdehyde
MTT	3-(4,5-Dimethylthiazol-2-yl)-2,5-Diphenyltetrazolium Bromide
NF-κB	Nuclear Factor Kappa-Light-Chain-Enhancer of Activated B Cells
NO	Nitric Oxide
PI	Propidium Iodide
ROS	Reactive Oxygen Species
SOD	Superoxide Dismutase
ZP	Zeta Potential

Author Contributions

C.A.U.: Writing-original manuscript draft, Formal analysis, Investigation, and Methodology; M.Z.L. and H.B.Y.: Validation, Investigation, and Conceptualization; M.Z.L. and T.S.M.: Data analysis, Editing, Review, and Validation; C.A.U.: Data analysis, Resources, and Visualizations; H.B.Y.: Validation and Supervision. All authors approved the final manuscript for submission.

Availability of Data and Materials

All data and figures analyzed during this study are included in this article (or available in the cited references).

Ethics Committee Approval

The study did not involve human participants or animal models. The MCF-7 and A549 cell lines used in this research were obtained from the American Type Culture Collection (ATCC, USA) and handled according to institutional research committee guidelines.

Consent for Publication

No consent for publication is required, as the manuscript does not involve any individual personal data, images, videos, or other materials that would necessitate consent.

Conflicts of Interest

The authors declare no conflicts of interest.

Funding

The study did not receive any external funding and was conducted using only institutional resources.

Acknowledgments

The authors are grateful to Emmanuel Dike of the National Steel Raw Material Exploration Agency, Kaduna, Nigeria, for his expertise in scanning electron microscopy used in this study. The manuscript grammar was improved using grammar editing and paraphrasing AI such as Grammarly within the permissible limits. The figures were computed using Python and, in some cases, GraphPad Prism version 8.

References

- [1] Mi, Q.; Shu, S.; Yang, C.; Gao, C.; Zhang, X.; Luo, X.; Bao, C.; Zhang, X.; Niu, J. Current Status for Oral Platinum (IV) Anticancer Drug Development. *Int. J. Med. Phys. Clin. Eng. Radiat. Oncol.* **2018**, *7*, 231–247. [[CrossRef](#)]
- [2] Mongalo, N.; Soyingbe, O.; Makhafa, T. Antimicrobial, Cytotoxicity, Anticancer and Antioxidant Activities of *Jatropha Zeyheri* Sond. Roots (Euphorbiaceae). *Asian Pac. J. Trop. Biomed.* **2019**, *9*, 307–314. [[CrossRef](#)]
- [3] Zhao, H.; Wu, L.; Yan, G.; Chen, Y.; Zhou, M.; Wu, Y.; Li, Y. Inflammation and Tumor Progression: Signaling Pathways and Targeted Intervention. *Signal Transduct. Target. Ther.* **2021**, *6*, 263. [[CrossRef](#)]
- [4] Kandilarov, I.; Gardjeva, P.; Georgieva-Kotetarova, M.; Zlatanova, H.; Vilmosh, N.; Kostadinova, I.; Katsarova, M.; Atliev, K.; Dimitrova, S. Effect of Plant Extracts Combinations on TNF-α, IL-6 and IL-10 Levels in Serum of Rats Exposed to Acute and Chronic Stress. *Plants* **2023**, *12*, 2–17. [[CrossRef](#)]
- [5] Li, S.; Zhang, H.; Chen, K.; Jin, M.; Vu, S.H.; Jung, S.; He, N.; Zheng, Z.; Lee, M.S. Application of Chitosan/Alginate Nanoparticle in Oral Drug Delivery Systems: Prospects and Challenges. *Drug Deliv.* **2022**, *29*, 1142–1149. [[CrossRef](#)] [[PubMed](#)]
- [6] Lee, Y.M.; Son, E.; Kim, S.H.; Kim, O.S.; Kim, D.S. Anti-Inflammatory and Anti-Osteoarthritis Effect of Mollugo Pentaphylla Extract. *Pharm. Biol.* **2019**, *57*, 74–81. [[CrossRef](#)]
- [7] Maroyi, A. *Maerua Angolensis* DC. (Capparaceae): A Review of Its Medicinal Uses, Phytochemistry and Pharmacological Properties. *J. Pharm. Nutr. Sci.* **2020**, *10*, 247–256. [[CrossRef](#)]
- [8] Li, J.; Cai, C.; Li, J.; Li, J.; Sun, T.; Wang, L.; Wu, H.; Yu, G. Chitosan-Based Nanomaterials for Drug Delivery. *Molecules* **2018**, *23*, 2661. [[CrossRef](#)] [[PubMed](#)]
- [9] Ukwubile, C.; Ahmed, A.; Katsayal, U.; Ya'u, J. In Vitro Anticancer Activity of Melastomastrum Capitatum Fern. Loaded Chitosan Nanoparticles on Selected Cancer Cells. *Drug Discov.* **2019**, *13*, 46–54. Available online: http://www.discoveryjournals.org/drugdiscovery/current_issue/2019/ (accessed on 7 February 2025).
- [10] Anjali, S.; Sindhu, R.; Rajeshkumar, S.; Nishitha, A. Anti Inflammatory Activity of Chitosan Nanoparti-

- cles With Chlorhexidine- An In vitro Study. *J. Popl. Ther. Clin. Pharmacol.* **2023**, *30*, 26–32. [[CrossRef](#)]
- [11] Mohammed, H.; Karhib, M.M.; Al-Fahad, K.S.J.; Atef, A.M.; Eskandrani, A.; Darwish, A.A.-E.; Sary, A.A.; Elwakil, B.H.; Bakr, B.A.; Eldrieny, A.M. Newly synthesized chitosan nanoparticles loaded with caffeine/moringa leaf extracts halt Her2, BRCA1, and BRCA2 expressions. *Sci. Rep.* **2024**, *14*, 18118. [[CrossRef](#)]
- [12] Ukwubile, C.A.; Ahmed, A.; Katsayal, U.A.; Ya, J.; Nettoy, H. Pharmacological Research—Natural Products Chitosan Nanoparticle-Mediated Drug Delivery for Linoleic Acid Isolated from *Melastomastrium Capitatum* Fern. Leaf Extract against MCF-7 and OV7 Cancer Cells. *Pharmacol. Res.-Nat. Prod.* **2024**, *5*, 100105. [[CrossRef](#)]
- [13] Selvaraj, H.; Periyannan, K.; Balachandar, S. Extraction and Characterization of Chitosan from the Shell Wastes of Indian Shrimp Using Different Methods of Deacetylation. *Indian J. Sci. Technol.* **2023**, *16*, 1118–1125. [[CrossRef](#)]
- [14] Desai, K.G.H.; Park, H.J. Preparation and Characterization of Drug-Loaded Chitosan-Tripolyphosphate Microspheres by Spray Drying. *Drug Dev. Res.* **2005**, *64*, 114–128. [[CrossRef](#)]
- [15] Ghannam, H.E.; Talab, A.S.; Dolgano, N.V.; Husse, A.M.S.; Abdelmagui, N.M. Characterization of Chitosan Extracted from Different Crustacean Shell Wastes. *J. Appl. Sci.* **2016**, *16*, 454–461. [[CrossRef](#)]
- [16] Alam, F.; Din, K.M.; Rasheed, R.; Sadiq, A.; Jan, M.S.; Minhas, A.M.; Khan, A. Phytochemical Investigation, Anti-Inflammatory, Antipyretic and Antinociceptive Activities of *Zanthoxylum Armatum* DC Extracts-in Vivo and in Vitro Experiments. *Helvion* **2020**, *6*, e05571. [[CrossRef](#)]
- [17] Borquaye, L.S.; Laryea, M.K.; Gasu, E.N.; Boateng, M.A.; Baffour, P.K.; Kyeremateng, A.; Doh, G. Anti-Inflammatory and Antioxidant Activities of Extracts of *Reissantia Indica*, *Cissus Cornifolia* and *Grosseria Vignei*. *Cogent Biol.* **2020**, *6*, 1785755. [[CrossRef](#)]
- [18] Bai, X.; Li, Y.; Li, Y.; Li, M.; Luo, M.; Tian, K.; Jiang, M.; Xiong, Y.; Lu, Y.; Li, Y.; et al. Antinociceptive Activity of Doliroside B. *Pharm. Biol.* **2023**, *61*, 201–212. [[CrossRef](#)]
- [19] Onyancha, J.M.; Gikonyo, N.K.; Wachira, S.W.; Mwitari, P.G.; Gicheru, M.M. Anticancer Activities and Safety Evaluation of Selected Kenyan Plant Extracts against Breast Cancer Cell Lines. *J. Pharmacogn. Phyther.* **2018**, *10*, 21–26. [[CrossRef](#)]
- [20] Kotowski, U.; Heiduschka, G.; Kadletz, L.; Fahim, T.; Seemann, R.; Schmid, R.; Schneider, S.; Mitterbauer, A.; Thurnher, D. Effect of Thymoquinone on Head and Neck Squamous Cell Carcinoma Cells in Vitro: Synergism with Radiation. *Oncol. Lett.* **2017**, *14*, 1147–1151. [[CrossRef](#)] [[PubMed](#)]
- [21] Aljutaily, T.; Almutairi, S.M.; Alharbi, H.F. The Nephroprotective Potential of *Brassica Nigra* Sprout Hydroalcoholic Extract against Carbon Tetrachloride-Induced Renal Toxicity in Rats. *Food* **2023**, *12*, 3906. [[CrossRef](#)] [[PubMed](#)]
- [22] Jaiswal, S.K.; Rao, C.V.; Sharma, B.; Mishra, P.; Das, S.; Dubey, M.K. Gastroprotective Effect of Standardized Leaf Extract from *Argyrea speciosa* on Experimental Gastric Ulcers in Rats. *J. Ethnopharmacol.* **2011**, *137*, 341–344. [[CrossRef](#)]
- [23] Mohammed, A.; Usman, M.I.; Wudil, A.M.; Alhasan, A.J.; Abubakar, S.M.; Lat, N.A. In Vitro and in Vivo Antioxidant Properties of Extracts from the Root of *Curcuma Longa* Linn. *European J. Med. Plants* **2020**, *31*, 6–12. [[CrossRef](#)]
- [24] Onyeto, C.A.; Onwuka, A.M.; Peter, I.E.; Nworu, C.S.; Akah, P.A. Effect of Aqueous Extract of Unripe *Musa Paradisiaca* Linn on Parameters Affecting Reproduction in Rats. *J. Evid.-Based Integr. Med.* **2024**, *29*, 1–9. [[CrossRef](#)] [[PubMed](#)]
- [25] Alfuraydi, A.A.; Aziz, I.M.; Almajhdi, F.N. Assessment of Antioxidant, Anticancer, and Antibacterial Activities of the Rhizome of Ginger (*Zingiber Officinale*). *J. King Saud Univ.-Sci.* **2024**, *36*, 103112. [[CrossRef](#)]
- [26] Saeed, M.M.; Fernández-Ochoa, Á.; Saber, F.R.; Sayed, R.H.; Cádiz-Gurrea, M.d.I.L.; Elmotayam, A.K.; Leyva-Jiménez, F.J.; Segura-Carretero, A.; Nadeem, R.I. The Potential Neuroprotective Effect of *Cyperus Esculentus* L. Extract in Scopamine-Induced Cognitive Impairment in Rats: Extensive Biological and Metabolomics Approaches. *Molecules* **2022**, *27*, 7118. [[CrossRef](#)]
- [27] Ojo, O.A.; Amanze, J.C.; Oni, A.I.; Grant, S.; Iyobhebe, M.; Elebiyo, T.C.; Rotimi, D.; Asogwa, N.T.; Oyinloye, B.E.; Ajiboye, B.O.; et al. Antidiabetic Activity of Avocado Seeds (*Persea Americana* Mill.) in Diabetic Rats via Activation of PI3K/AKT Signaling Pathway. *Sci. Rep.* **2022**, *12*, 2919. [[CrossRef](#)]
- [28] Ghosh, S.; Das, S.K.; Sinha, K.; Ghosh, B.; Sen, K.; Ghosh, N.; Sil, P.C. The Emerging Role of Natural Products in Cancer Treatment. *Arch. Toxicol.* **2024**, *98*, 2353–2391. [[CrossRef](#)]
- [29] Fang, G.; Zhang, A.; Zhu, L.; Wang, Q.; Sun, F.; Tang, B. Nanocarriers Containing Platinum Compounds for Combination Chemotherapy. *Front. Pharmacol.* **2022**, *13*, 1050928. [[CrossRef](#)]
- [30] Nelson, V.K.; Sahoo, N.K.; Sahu, M.; Sudhan, H.h.; Pullaiah, C.P.; Muralikrishna, K.S. In Vitro Anticancer Activity of *Eclipta Alba* Whole Plant Extract on Colon Cancer Cell HCT-116. *BMC Complement. Med. Ther.* **2020**, *20*, 355. [[CrossRef](#)]
- [31] Zeng, M.; Zhu, L.; Li, L.; Kang, C. MiR-378 Suppresses the Proliferation, Migration and Invasion of Colon Cancer Cells by Inhibiting SDAD1. *Cell. Mol. Biol. Lett.* **2017**, *22*, 12. [[CrossRef](#)]
- [32] Zhang, H.; Park, S.; Huang, H.; et al. Anticancer effects and potential mechanisms of ginsenoside Rh2 in various cancer types. *Oncol. Rep.* **2021**, *45*, 33. [[CrossRef](#)]
- [33] Javid, A.; Ahmadian, S.; Saboury, A.A.; Kalantar, S.M.; Rezaei-Zarchi, S. Chitosan-Coated Superparamagnetic Iron Oxide Nanoparticles for Doxorubicin Delivery: Synthesis and Anticancer Effect against

- Human Ovarian Cancer Cells. *Chem. Biol. Drug Des.* **2013**, *82*, 296–306. [[CrossRef](#)]
- [34] Deng, Z.; Wang, N.; Ai, F.; Wang, Z.; Zhu, G. Nanomaterial-Mediated Platinum Drug-Based Combinatorial Cancer Therapy. *View* **2021**, *2*, 1–22. [[CrossRef](#)]
- [35] Vllasaliu, D.; Casettari, L.; Bonacucina, G.; Cespi, M.; Palmieri, G.; Illum, L. Folic Acid Conjugated Chitosan Nanoparticles for Tumor Targeting of Therapeutic and Imaging Agents. *Pharm. Nanotechnol.* **2013**, *1*, 184–203. [[CrossRef](#)]
- [36] Perrone, D.; Ardito, F.; Giannatempo, G.; Dioguardi, M.; Troiano, G.; Lo Russo, L.; De Lillo, A.; Laino, L.; Lo Muzio, L. Biological and Therapeutic Activities, and Anticancer Properties of Curcumin (Review). *Exp. Ther. Med.* **2015**, *10*, 1615–1623. [[CrossRef](#)] [[PubMed](#)]
- [37] Mehrotra, S.; Goyal, V.; Dimkpa, C.O.; Chhokar, V. Green Synthesis and Characterization of Ginger-Derived Silver Nanoparticles and Evaluation of Their Antioxidant, Antibacterial, and Anticancer Activities. *Plants* **2024**, *13*, 1255. [[CrossRef](#)] [[PubMed](#)]